An Empirical Study of the Relationship between Lyα and UV selected Galaxies: Do Theorists and Observers 'Select' the Same Objects?

Mark Dijkstra[1]* and J. Stuart B. Wyithe[2]

[1] *Max Planck Institute for Astrophysics, Karl-Schwarzschild-Str. 1, 85741, Garching, Germany*
[2] *School of Physics, University of Melbourne, Parkville, Victoria, 3010, Australia*

22 August 2011

ABSTRACT

Lyman Alpha Emitters (LAEs) are galaxies that have been selected on the basis of a strong Lyα emission line in their spectra. Observational campaigns over the last decade have dramatically increased the sample of known LAEs, which now extends out to $z = 7$. These discoveries have motivated numerous theoretical studies on the subject, which usually define LAEs in their models based on sharp Lyα luminosity and equivalent width (EW) cuts. While broadly representative, this procedure does not mimic the selection from observational programs in detail, which instead use cuts in various colour-spaces. In this paper we investigate what implications this disjoint may have for theoretical studies that aim to model the observed population of LAEs. We construct an empirical model for the number density of star forming galaxies as a function of their UV and Lyα luminosity, utilising measured constraints on the luminosity functions of drop-out galaxies, and their luminosity dependent probability distribution function of Lyα EW. In particular, we investigate whether the LAE luminosity functions can be reproduced by defining LAEs using a (z-dependent) Lyα luminosity and EW threshold. While we are able to reproduce the observed distribution of Lyα EW among LAEs out to restframe EW$\sim$ 200 Å, we find that our formalism *over-predicts* both the UV and Lyα luminosity functions of LAEs by a factor of 2-3, and is inconsistent with observations at the $\sim 95\%$ level. This tension is partially resolved if we assume the Lyα EW-distribution of drop-out galaxies to be truncated at restframe EW $\gtrsim$150 Å. However the overprediction indicates that modeling LAEs with simple REW and luminosity cuts does not accurately mimic observed selection criteria, and can therefore lead to uncertainties in the predicted number density of LAEs. On the other hand, the predicted redshift evolution is not affected. We apply our formalism to drop-out galaxies at $z > 6$, and predict the luminosity functions of LAEs at $z = 7 - 9$.

Key words: galaxies: high redshift – galaxies: high-redshift – galaxies: luminosity functions – line: formation – radiative transfer – scattering

1 INTRODUCTION

Two complementary observational techniques have been very succesful in finding high-redshift galaxies. The Lyman Break technique – or drop-out technique – has been used to constrain the observed rest-frame UV luminosity functions of Lyman Break galaxies (LBGs) out to redshifts as high as $z = 10$ (e.g. Bouwens et al. 2010a; Bunker et al. 2010; Finkelstein et al. 2010; Yan et al. 2010; Oesch et al. 2011). The Lyman Break technique relies on the fact that the spectra of star forming galaxies are strongly suppressed blue-ward of the Lyman-α resonance at $\lambda \lesssim$1216 Å (Steidel et al. 1996). The presence of this 'break' in the spectrum is a direct consequence of the temperature of stellar atmospheres, and of the interstellar and intergalactic absorption of ionizing and Lyman series photons. The resulting break in the spectrum strongly suppresses the broad-band flux blueward of some–redshift dependent–filter that is observed from a galaxy (i.e. V drop-out galaxies at $z \sim 5$ are detected only in filters redder than V).

Narrowband surveys have constrained luminosity functions of Lyα emitting galaxies (a.k.a Lyα emitters, or LAEs) out to $z \sim 9$ (Hu et al. 2002; Iye et al. 2006; Ouchi et al. 2008, 2010; Willis et al. 2008; Hibon et al. 2010; Tilvi et al.

* E-mail:dijkstra@mpa-garching.mpg.de

2010; Clément et al. 2011), while Lehnert et al. (2010) have also reported discovery of a Y_{105} drop-out galaxy with strong Lyα emission. The narrow band technique relies on the presence of a strong Lyα emission line, which mostly originates in galactic HII regions (Partridge & Peebles 1967). The presence of such a line can produce an excess of observed flux in a narrowband filter (FWHM$\sim$ 100 Å) that is larger than expected based on the observed flux in overlapping broadband filters (e.g. Rhoads et al. 2000).

Existing observations have given us accurate determinations of the luminosity functions of LBGs and LAEs. The observed rest-frame UV luminosity function of drop-out galaxies decreases monotonically with redshift at $z \geqslant 3$ (e.g. Reddy & Steidel 2009; Bouwens et al. 2006, 2007, 2008). These luminosity functions can be converted into a cosmic star formation rate density, which drops by more than an order of magnitude between $z = 3$ and $z > 6$ (e.g. Hopkins & Beacom 2006; Bouwens et al. 2009; Robertson et al. 2010). Furthermore, the broad band colours of drop-out galaxies become bluer with redshift, which indicates that star forming galaxies become increasingly dust-free (Stanway et al. 2005; Bouwens et al. 2010b; Finkelstein et al. 2010).

The redshift evolution of the luminosity function of LAEs is different. The Lyα luminosity functions of LAEs are observed to be remarkably constant between $z = 3$ and $z = 6$ (e.g. Hu et al. 1998; Ouchi et al. 2008), after which the number density decreases at $z \gtrsim 6$ (Kashikawa et al. 2006; Ota et al. 2008, 2010; Kashikawa et al. 2011, but also see Hu et al. 2010). The first of these observations may be another consequence of the decreasing dust content of star forming galaxies towards higher redshift (Hayes et al. 2011; Blanc et al. 2011). The second observation has received significantly more attention because it may signpost the existence of large regions of intervening neutral intergalactic gas, which are opaque to the Lyα photons (Haiman & Spaans 1999; Malhotra & Rhoads 2006; Kashikawa et al. 2006). However, a proper interpretation of the redshift evolution of LAE luminosity functions at all redshifts requires understanding the detailed radiative transfer of Lyα photons through both the interstellar medium (Santos 2004; McQuinn et al. 2007; Dijkstra & Wyithe 2010; Barnes et al. 2011; Dijkstra et al. 2011), and ionized intergalactic medium (e.g. Dijkstra et al. 2007b; McQuinn et al. 2007; Iliev et al. 2008; Zheng et al. 2010a; Dayal et al. 2011; Laursen et al. 2011; Dijkstra et al. 2011, also see e.g. Fernandez & Komatsu 2008).

LAEs are selected differently in theoretical models and observations. Observationally, LAEs are defined by their location in several 2-dimensional color-colour spaces. For example, Ouchi et al. (2008) define $z = 3.1$ LAEs by requiring that $V - NB503 > 1.2$ and $[(V < V_{2\sigma}$ and $B - V > 0.5)$ or $(V \geqslant V_{2\sigma}$ and $B - V_{2\sigma} > 0.5)$, where $V_{2\sigma} = 27.7$ denotes the 2σ limiting magnitude of the V-band images]. The first requirement corresponds to having an excess flux in the narrowband filter denoted by NB503, while the broad-band selection corresponds to the requirement of having break in the spectrum blueward of the Lyα resonance. The requirement that the object have a strong narrowband excess translates *approximately* to a minimum restframe equivalent width (REW$_{min}$) of the Lyα line. In detail REW$_{min}$ depends on the S/N at which an object is detected (see e.g. Gronwall

et al. 2007 for an extended discussion on this and other complications regarding the flux dependence of the survey volume). Representative values of REW$_{min}$ are often reported in papers discussing measurements of the LAE luminosity function, but these numbers should be interpreted with caution (e.g. Ouchi et al. 2008). However, when describing the LAE population in numerical or semi-analytic calculations, theoretical models generally literally adopt the quoted minimum values of REW$_{min}$ to select LAEs from model galaxies (e.g. Le Delliou et al. 2006; Dijkstra et al. 2007a; Mao et al. 2007; McQuinn et al. 2007; Kobayashi et al. 2010; Nagamine et al. 2010; Dayal et al. 2011; Zheng et al. 2010a; Shimizu et al. 2011; Forero-Romero et al. 2011). In addition, some theoretical papers only apply flux thresholds, which formally separates them further from observations.

In this paper, we investigate the impact of simplified selection criteria (i.e. joint REW and luminosity cuts) on the 'predicted' number density of LAEs. In particular, we generate phenomenological models for the number density of star forming galaxies as a function of UV and Lyα luminosity. We then investigate whether we can reproduce the LAE data if we define LAEs by a (redshift dependent) Lyα luminosity and equivalent width (EW) threshold. Our empirical models are taken from observed drop-out luminosity functions at $3 \leqslant z \leqslant 6$, combined with observational constraints on the prominence of Lyα emission lines in drop-out galaxies. The Lyα equivalent width distribution for LBGs has been measured at $z = 3$ by Shapley et al. (2003), and at $3 < z < 7$ for a slightly smaller sample by Stark et al. (2010, 2011). We then investigate whether it is possible to reproduce the observed Lyα luminosity functions (i.e. the number density of LAEs as a function of Lyα luminosity and UV magnitude) and equivalent width distributions, based solely on our knowledge of this LBG population. If this is not possible, then the analysis implies that utilising simplified selection criteria can have a strong impact on the predicted number of LAEs. Indeed, our results indicate that as models of LAEs mature, selection criteria that resemble those applied on the actual data will increasingly have to be taken into consideration.

The outline of our paper is as follows: in § 2 we describe our formalism for 'predicting' the Lyα luminosity function, and its uncertainties. In § 3 we present our results for Lyα luminosity functions at $z \lesssim 7$, and provide a discussion of uncertainties in § 4. We also make predictions for LAE luminosity functions out to $z = 10$ in § 5. Finally, in § 6 we present our conclusions. The cosmological parameter values used throughout our discussion are $(\Omega_m, \Omega_\Lambda, \Omega_b, h) = (0.27, 0.73, 0.046, 0.70)$ (Komatsu et al. 2009).

2 EMPIRICAL RELATIONSHIP BETWEEN LBGS AND LAES

The range of UV-magnitudes probed by samples of LBG and LAEs[1] currently overlap. Furthermore, recent Lyα radiative transfer modeling shows that Lyα photons escape anisotropically from young, dusty, simulated galaxies (Laursen et al. 2009). This implies that the observed narrow-band excess of a star forming galaxy – and hence, whether it would be

---

[1] For many LAEs the UV continuum is also detected.

selected into a sample of LAEs – depends on its orientation relative to the observer. Furthermore, modelling of the observed spectral profiles of LBGs near the Lyα line suggests that LBGs observed not to have any Lyα emission are not a separate class of galaxy. Rather, these are also intrinsically strong Lyα emitters, in which radiative transfer effects transform the Lyα emission line into an absorption feature (Schaerer & Verhamme 2008; Atek et al. 2009; Dessauges-Zavadsky et al. 2010)[2]. Together these observations indicate that the LBG and LAE populations are intrinsically the same, and are only separated as a consequence of Lyα radiative transfer through opaque (dusty) media.

The possibility that Lyα radiative transfer plays an important role in separating LAEs from LBGs is underlined by the observation of low surface brightness, extended Lyα halos around LBGs (Steidel et al. 2011). Steidel et al. (2011) argue that the Lyα radiation in these halos was emitted as nebular emission, which is then scattered to the observer in the (outflowing) circumgalactic medium. When the flux in these halos is properly accounted for, the total observed Lyα flux places most LBGs in the LAE category.

Thus, current evidence suggests that the LBG and LAE populations should be considered within the same theoretical framework. However, before this can be reliably pursued it is important to understand the observational selection criteria that define LAEs.

2.1 The Formalism

Our goal is to connect the observed numbers of LAEs and LBGs. In this section we therefore begin by introducing the formalism used in this paper. The number density of LAEs with Lyα luminosities in the range $L_\alpha \pm dL_\alpha/2$ is

$$
\begin{aligned}
\Phi(L_\alpha)dL_\alpha = & \ dL_\alpha \times F \times (1+\delta_V) \times \\
& \int_{M_{\min}}^{M_{\max}} dM_{\mathrm{uv}} \phi(M_{\mathrm{uv}}) P(L_\alpha|M_{\mathrm{uv}}),
\end{aligned}
\tag{1}
$$

where $\phi(M_{\mathrm{uv}})dM_{\mathrm{UV}}$ denotes the number density of galaxies with absolute AB-magnitude range $M_{\mathrm{uv}} \pm dM_{\mathrm{UV}}$, and $P(L_\alpha|M_{\mathrm{uv}})$ is the conditional probability density function (PDF) for L_α for a given M_{UV}. The parameter F is a normalisation factor which is discussed in § 2.3. The factor $(1+\delta_V) \equiv \Delta_V$ accounts for cosmic variance, and we assume that Δ_V is drawn from a Gaussian distribution with a standard deviation $\sigma_V = 0.36$ (estimated following the procedure of Somerville et al. 2004, see Moster et al. 2011 for an update of this work)[3]. The integral is taken over the range $M_{\min} = -30.0$ to $M_{\max} = -12.0$.

---

[2] How frequently such a 'transformation' occurs can depend on the metallicity of the interstellar gas (e.g. Finkelstein et al. 2011).
[3] The cosmic variance recipe given by Somerville et al (2004) formally applies to spherical volumes. The narrowband survey of Ouchi et al. (2008) probes volumes that are close to cubical, and therefore Somerville et al. (2004) should provide reasonable estimates for their cosmic variance. For the appropriate survey volume of $0.5 - 0.9 \times 10^6$ Mpc^{-3}, Figure 3 of Somerville et al. (2004) gives $\sigma_{\mathrm{DM}} = 0.03 - 0.06$. To get a conservatively large estimate for σ, we adopt a linear bias parameter of $b = 6$ which is on the high end of the observed range (e.g. Shimasaku et al. 2003; Gawiser et al. 2007; Kovač et al. 2007; Guaita et al. 2010). This gives us $\sigma \sim 0.18 - 0.36$.

Table 1. Adopted parameters for $\phi(M_{\mathrm{uv}})$.

redshift	ϕ^* (10^{-3} cMpc^{-3})	M^*_{UV}	α
$z = 3^a$	1.7 ± 0.5	-21.0 ± 0.1	-1.73 ± 0.13
$z = 4^b$	1.3 ± 0.2	-21.0 ± 0.1	-1.73 ± 0.05
$z = 6^b$	$1.4^{+0.6}_{-0.4}$	-20.2 ± 0.2	-1.74 ± 0.16
$z = 7^c$	$1.1^{+1.7}_{-0.7}$	-19.8 ± 0.4	-1.74
$z = 8^d$	$1.1^{+1.7}_{-0.7}$	-19.45	-1.74
$z = 9^c$	$1.1^{+1.7}_{-0.7}$	$\gtrsim -19.6$	-1.74

[a] From Reddy & Steidel (2009).
[b] From Bouwens et al. (2007).
[c] From Bouwens et al. (2008). The slope α was kept fixed at the value that was inferred from the lower redshift observations. To obtain the lower limit on M^*_{UV}, the value for ϕ^* at $z = 9$ was assumed to be the same as at redshift 7.
[d] From Bouwens et al. (2010a). The constraint on M^*_{UV} was obtained by assuming no evolution in ϕ^* and α.

Table 2. Parameters related to detection thresholds in the narrowband surveys.

redshift	REW$_{\min}$[a]	$L_{\alpha,\min/\max}$ $(\frac{\mathrm{erg}}{\mathrm{s}})$[b]
$z = 3.1$	64 Å	2 / 50$\times 10^{42}$
$z = 3.7$	44 Å	4 / 40$\times 10^{42}$
$z = 5.7$	27 Å	2.5 / 40$\times 10^{42}$

[a] Taken from Table 3 of Ouchi et al. (2008).
[b] The Lyα luminosity functions of Ouchi et al. (2008) has bins with a width of 0.2 dex (in $\log_{10} L_\alpha$). To estimate $L_{\alpha,\min}$ ($L_{\max}$), we subtracted (added) 0.1 dex from (to) the Lyα luminosity of the faintest (brightest) bin.

2.1.1 The Drop-Out Luminosity Function $\phi(M_{\mathrm{uv}})dM_{\mathrm{UV}}$

We assume that the LBG luminosity function $\phi(Muv)dM_{\mathrm{uv}}$ is described by a Schechter function, the parameters of which $(\phi^*, M^*_{\mathrm{UV}}, \alpha)$ we take from the literature. Table 1 summarizes the redshift dependence of our adopted parameters, and the references from which these were taken. Note that formally, the Lyα luminosity functions have been determined at $z = 3.1$, $z = 3.7$ and $z = 5.7$. We have interpolated the UV luminosity functions to these same redshifts by assuming that M^*_{UV} evolves as $M^*_{\mathrm{UV}} = -21.02 + 0.36(z - 3.8)$ (Bouwens et al. 2008) while keeping the other parameters fixed.

2.1.2 The Conditional Probability $P(L_\alpha|M_{\mathrm{uv}})$

The absolute AB UV-magnitude relates to the UV luminosity density $L_{\mathrm{UV},\nu}$ (in erg s^{-1} Hz^{-1}) as $M_{\mathrm{UV}} = -2.5 \log L_{\mathrm{UV},\nu} + 51.6$ (Ouchi et al. 2008). Because Lyα luminosity is simply the product of rest frame equivalent width (REW) and luminosity density (L$_\lambda$ in erg s^{-1} Å^{-1}), we can express Lyα luminosity as a function of REW and $L_{\mathrm{UV},\nu}$ as $L_\alpha = C \times \mathrm{REW} \times L_{\mathrm{UV},\nu}$. The constant $C \equiv \frac{\nu_\alpha}{\lambda_\alpha}\left(\frac{\lambda_{\mathrm{UV}}}{\lambda_\alpha}\right)^{-\beta-2}$, in which $\nu_\alpha = 2.47 \times 10^{15}$ Hz, $\lambda_\alpha = 1216$ Å, $\beta \equiv d \log L_\lambda / d \log \lambda$ (i.e. $L_\lambda \propto \lambda^\beta$ and $L_\nu \propto \nu^{-\beta-2}$), and $\lambda_{\mathrm{UV}} =$

1700 Å denotes the restframe wavelength at which the UV continuum flux density was measured (Dijkstra & Westra 2010). Throughout this work we assume $\beta = -1.7$ (see § 4.2). We can thus recast the conditional probability $P(L_\alpha|M_{uv})$ as a function of the REW-PDF as

$$P(L_\alpha|M_{uv}) = \left\{ \begin{array}{ll} P(x|M_{UV})\frac{\partial REW}{\partial L_\alpha} & x \in (x_{min}, x_{max}); \\ 0 & \text{otherwise,} \end{array} \right. \quad (2)$$

where $x \equiv REW = L_\alpha/[C \times L_{UV,\nu}]$, and x_{min} denotes the minimum equivalent width REW_{min} that a given narrowband survey is sensitive to (for smaller values of REW the narrow band excess would be too small for the galaxy to make it into the sample of LAEs). Numerical values of $x_{min} \equiv REW_{min}$ that approximately represent the colorcuts adopted by Ouchi et al. (2008, see their Table 23) are given in Table 2. For the maximum REW we have assumed $x_{max} \equiv REW_{max} = 300$ Å, but note that our results do not depend precisely on this number (see § 4.2).

The conditional PDF for the REW $[P(REW|M_{UV})]$ has been measured for LBGs. In Appendix A1 we show that the Lyα REW PDF can be well described by an exponential whose scale length depends on M_{UV} and z

$$P(REW|M_{UV}) = \mathcal{N}\exp\left(\frac{-REW}{REW_c(M_{UV})}\right), \quad (3)$$

where $\mathcal{N}$ denotes a normalization constant, and $REW_c(M_{UV}) = REW_{c,0} + \frac{dREW_c}{dM_{UV}}\Delta M + \frac{dREW_c}{dz}\Delta z$ with $\Delta M \equiv M_{UV} + 21.9$, and $\Delta z = z - 4.0$. In this expression the factor $a_1 = 20$ Å for $M_{UV} < -21.5$, and $a_1 = 20 - 6(M_{UV} - 21.5)^2$ Å for $-21.5 \leqslant M_{UV} \leqslant -19.0$, and we freeze the evolution of a_1 for $M_{UV} > -19.0$. The best fit values are $REW_{c,0} = 22 \pm 3$ Å, and $\frac{dREW_c}{dM_{UV}} = 6 \pm 4$ Å. Equation (3) ensures that the fraction of drop-out galaxies with Lyα in emission (i.e. REW $\gtrsim 0$) depends on M_{UV}, as is observed. We assume throughout that this fitting formula applies only in the observed range of UV magnitudes, and also freeze the evolution of $REW_c(M_{UV})$ for $M_{UV} > -19.0$ (see § 4.2 for a discussion of the uncertainties this may introduce). The choice of the functional form that approximates the data is quite arbitrary. In Appendix A2 we investigate an alternative parametrization, and find that our results are not significantly affected.

2.2 Comparison to Data

We next compute 'predicted' Lyα luminosity functions by combining Eq 1, Eq 2, and Eq 3 at $z = 3.1$, $z = 3.7$ and $z = 5.7$. To facilitate the comparison with the data, we compute the quantity $\Psi(L_\alpha)d\log L_\alpha$ which denotes the number density of LAEs in the range $\log L_\alpha \pm (d\log L_\alpha)/2$. The units of $\Psi(L_\alpha)$ are cMpc^{-3} $[\log L_\alpha]^{-1}$, and we have $\Psi(L_\alpha) = \ln 10 L_\alpha \Phi(L_\alpha)$.

Each model is described by three parameters that quantify the Lyα REW distribution ($REW_{c,0}$, $\frac{dREW_c}{dM_{UV}}$, $\frac{dREW_c}{dz}$), the normalization parameter F, and three Schechter parameters plus one cosmic variance parameter at each redshift bin. We therefore need to explore a 16-dimensional parameter space $(3 + 1 + 3 \times 4 = 16)$, which we do with a Monte Carlo Markov Chain (MCMC) method. We characterize each model by the parameter vector $\mathbf{P} = (REW_{c,0}, \frac{dREW_c}{dM_{UV}}, \frac{dREW_c}{dz}$

$, F, \alpha_{3,..,6}, \phi^*_{3,...,6}, M^*_{UV,3,...,6}, \delta_{V,3,...,6})$. Here, we have adopted a notation where α_3 denotes the value of α at $z = 3$. We compute the posterior probability for each model as $P(\mathbf{P}) \propto \mathcal{L}[\mathbf{P}]P(\mathbf{P})$, where $\mathcal{L}[\mathbf{P}] = \exp[-0.5\chi^2]$ denotes the likelihood, in which $\chi^2 = \sum_i^{N_{data}}(model_i - data_i)^2/\sigma_i^2$. The function $P(\mathbf{P})$ denotes the prior PDF for these parameters (e.g. Cowan 1997).

We have assumed that $P(\mathbf{P})$ is a multivariate Gaussian, i.e. $P(\mathbf{P}) = \mathcal{N}\exp\left[-\frac{1}{2}(\mathbf{P} - \mu_P)^T \mathbf{C}^{-1}(\mathbf{P} - \mu_P)\right]$, where $\mathcal{N}$ denotes the normalization factor. The vector μ_P contains the best fit values for each of the parameters (e.g. from Table 1 we have $\mu_{\alpha,3} = -1.73$, and in § 2.1.2 we find that $\mu_{REW,c,0} = 22$ Å). Note that we do not assume any prior knowledge of F or $\frac{dREW}{dz}$. The covariance matrix $\mathbf{C}$ contains the measured uncertainties on the parameters[4]. Table 1 summarizes the assumed redshift evolution for M^*_{UV}, ϕ^* and α and their uncertainties. We then compute marginalized PDFs for the parameters F and $\frac{dREW}{dz}$ by marginalizing over the other 15 parameters. The data that we use for the fits is from Ouchi et al. (2008).

Finally, we summarize other model parameters that we do not vary as part of the MCMC calculations in Table 2. These parameters include: (i) the approximate minimum equivalent width (REW_{min}), and (ii) the minimum Lyα luminosity (L_α) to which the narrowband survey of Ouchi et al. (2008) was sensitive.

2.3 The 'normalization' parameter F

The 'normalization' parameter F scales the predicted luminosity function up and down, and so can be interpreted as the ratio of the observed to predicted number density of LAEs. In this paper we focus on the value of F that arrises from fitting to LAE and LBG luminosity functions, as a means of testing the validity of using a simple cut in Lyα luminosity and REW to represent the real observational selection criteria. In a case where the simple cuts accurately represent the true selection criteria (and hence models provide a faithful representation of the data) we therefore expect that $F = 1$. However any deviation of F from unity indicates that the simple cuts are not providing an adequate description of the observational selection criteria.

3 RESULTS

3.1 The Lyα Luminosity Functions

In Figure 1 we show Lyα luminosity functions at $z = 3.1$ (*upper left*), $z = 3.7$ (*middle*) and $z = 5.7$ (*upper right*). The

---

[4] The covariance matrix in this case is a 16×16 matrix whose entries are given by $C_{ij} = \sigma_i\sigma_j\rho_{ij}$. Here σ_i denotes the uncertainty on parameter 'i', and ρ_{ij} denotes the correlation coefficient between parameter i and j. While these correlation coefficients are generally not given, the constraints on the parameters α, M^*_{UV}, ϕ^* at a given redshift *are* strongly correlated. We assumed throughout that $\rho_{\alpha,M^*} = \rho_{M^*,\phi^*} = \rho_{\alpha,\phi^*} = 0.9$ at each redshift. We found that this decently reproduces the shape of the 68% and 95% likelihood contours for different Schechter parameter combinations as given by Bouwens et al. (2007). We assume that the other parameters are not correlated, i.e. $\rho_{ij} = 0$. By definition $\rho_{ii} = 1$ for all 'i'.
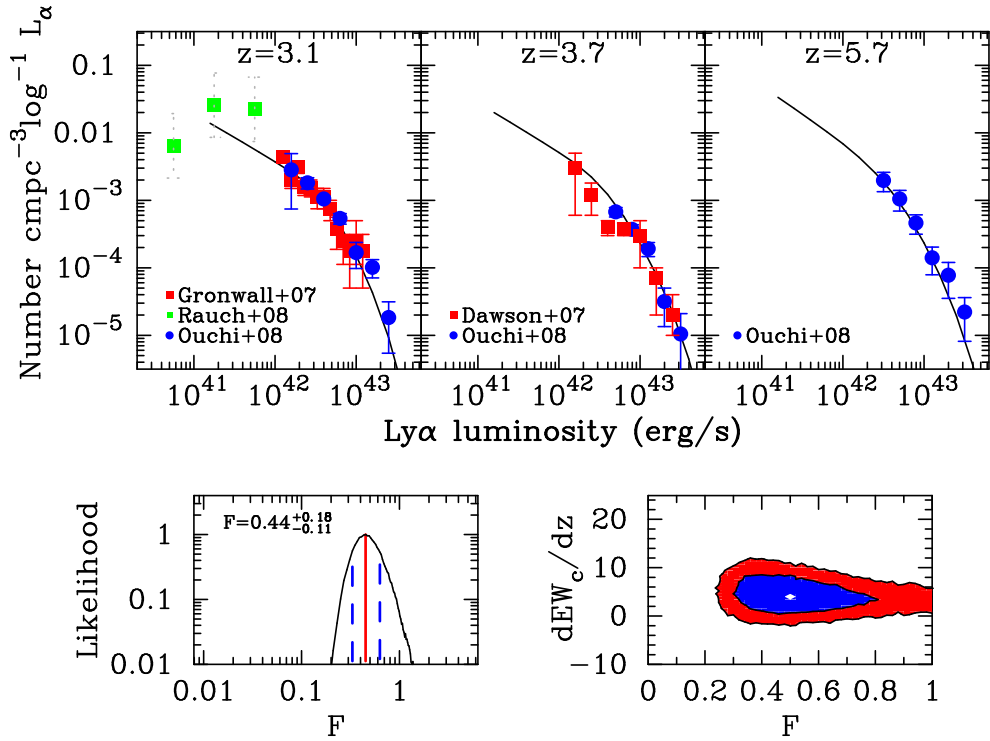
Figure 1. We plot Lyα luminosity functions at $z = 3.1$ (*upper left*), $z = 3.7$ (*middle*) and $z = 5.7$ (*upper right*). The *solid black lines* show our best fit model, which we calculated following the procedure described in § 2.1.1 -§ 2.2. The data of Ouchi et al. (2008) are indicated as *blue circles* in *all panels*. For completeness, we have also shown some other data sets, which were not included in our fits (see text). The *lower left panel* show marginalized posterior PDF for the parameter F. The *lower right panel* shows the 68% and 95% contours in the $F - \frac{d\text{REW}_c}{dz}$ plane, which we obtained by marginalizing over all other parameters.

Figure 2. The predicted UV luminosity function of LAEs for our best-fit model (*black solid lines*), compared to the data of Ouchi et al. (2008). The agreement between our model and the data is excellent at $z = 3.1$ (*left panel*, note that this is not a fit), and reasonable at $z = 3.7$ (*central panels*). Our model underpredicts the UV luminosity function at $z = 5.7$, which may be related a slight overabundance of large REW (REW $\gtrsim 200$ Å) systems in our model (see text). For completeness, we have also shown the best-fit drop-out galaxy luminosity function (*black dashed lines*), and the best fit Schechter function of the UV luminosity function of LAEs as derived by Ouchi et al. (2008, *red dotted lines*).

solid black lines show our best fit model (see below), which we calculated following the procedure described in § 2.1.1 -§ 2.2. The data of Ouchi et al. (2008) is indicated as *blue circles in all panels*. For completeness, we have also shown the $z = 3$ data from Rauch et al. (2008, *green circles*) and Gronwall et al. (2007, *red circles*), and the $z = 3.7$ data from

Dawson et al. (2008, *red squares*). These other data points were not included in our fits.

The best fit model is in excellent agreement with the data, and is described by the parameters $\text{REW}_{c,0} = 23$ Å, $\frac{d\text{REW}_c}{dM_{\text{UV}}} = 7$ Å, $\frac{d\text{REW}_c}{dz} = 6$ Å, $F = 0.53$, $\alpha_3 = -1.65$, $\phi_3^* = 1.9 \times 10^{-3}$ cMpc^{-3}, $M_{\text{UV},3}^* = -20.9$, $\delta_{\text{V},3} = +0.04$; $\alpha_4 = -1.70$, $\phi_4^* = 1.3 \times 10^{-3}$ cMpc^{-3}, $M_{\text{UV},4}^* = -20.9$, $\delta_{\text{V},4} = -0.10$,
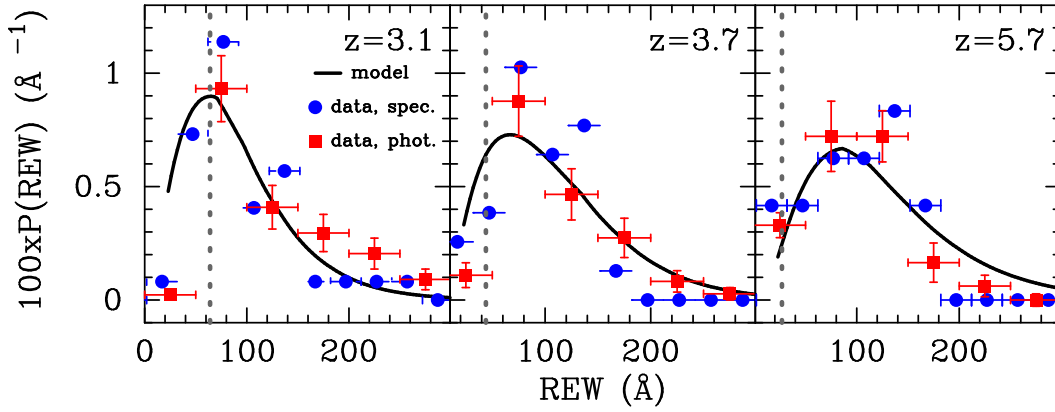
Figure 3. The model equivalent width PDF (*black thick solid lines*), compared to the best estimate of the observed REW PDF at $z = 3.1$, $z = 3.7$ and $z = 5.7$ (Ouchi et al. 2008), for all their photometrically selected LAEs (*red filled squares*), and for spectroscopically identified LAEs (*blue filled circles*). The *vertical dotted lines* indicate the minimum REW of the Lyα emission line that galaxies need to have in order to be selected as LAEs by Ouchi et al. (2008).

$\alpha_6 = -1.73$, $\phi_6^* = 1.5 \times 10^{-3}$ cMpc^{-3}, $M_{UV,6}^* = -20.4$, $\delta_{V,6} = 0.01$. It is interesting – though likely a coincidence – that this model is in reasonable agreement with the data of Rauch et al. (2008, *green circles*). These authors detected 27 ultrafaint Lyα emitters in a long-slit, 92 hrs, observation with the ESO VLT FORS2 spectrograph, and probed an effective volume of $\sim 10^3$ cMpc^3. In such a small volume cosmic variance is significant. Following the prescription of Somerville et al. (2004) for estimating cosmic variance, we find that the uncertainty on the number of detected galaxies is $\sigma_N \sim 0.8\langle N \rangle$. These uncertainties are denoted as *grey dashed lines* because this estimate is likely not accurate for the highly elongated survey volume probed by Rauch et al. (2008, see Muñoz et al. 2010 for a discussion of cosmic variance in pencil beam surveys).

The *lower left panel* shows the marginalized posterior PDF for the parameter F. Based on available data for the drop-out galaxy population we find that we *overpredict* the number density of LAEs, and so need to multiply our predictions by a constant factor of $F \sim 0.43$ to match the data. Formally, $F = 1$ is ruled out at $\sim 95\%$ CL. As noted previously, in a case where sharp REW and luminosity cuts among the population of drop-out galaxies can be used to reproduce the observed luminosity functions of LAEs we expect $F = 1$. The fact that the data are inconsistent with $F = 1$ therefore demonstrates that the use of sharp luminosity and REW cutoffs does not adequately describe the observational selection of LAEs. This represents the primary conclusion of our paper.

In the *lower right panel* we plot the 68% and 95% contours in the $F - \frac{dREW_c}{dz}$ plane, which we obtained by marginalizing over all other parameters. The data clearly prefer models with $\frac{dREW_c}{dz} > 0$, in excellent agreement with the findings of Stark et al. (2010, 2011, also see Fig 4).

3.2 The UV Luminosity Functions

We next take our best-fit model and compare it to other observed properties of LAEs. First, we 'predict' the UV luminosity function of LAEs, $\Phi_{LAE}(m_{UV}, z)$

$$\Phi_{LAE}(m_{UV}, z) = \phi(M_{uv}, z) \times \mathcal{F}(M_{UV}, z), \qquad (4)$$

where $\phi(M_{uv}, z)$ denotes the LBG UV luminosity function (introduced in § 2), and $\mathcal{F}(M_{UV}, z)$ denotes the fraction of drop-out galaxies that have REW$\geqslant$ REW$_{min}$ and a total Lyα flux greater than $L_{\alpha,min}$ (see Table 2 for numerical values of $L_{\alpha,min}$ and REW$_{min}$). Note that this latter constraint is important. For fainter drop-out galaxies, the requirement that the Ly-α flux be sufficiently large can translate to a higher required minimum REW (also see Zheng et al. 2010a). The fraction $\mathcal{F}(M_{UV}, z)$ is then obtained by integrating over the REW-PDF.

Figure 2 shows the best-fit drop-out galaxy luminosity function (*black dashed lines*), the best fit Schechter function of the UV luminosity function of LAEs as derived by Ouchi et al. (2008, *red dotted lines*), and our predicted UV luminosity function of LAEs for the best-fit model shown in Figure 1 (*black solid lines*). The 'breaks' in the UV-luminosity functions at $M_{UV} > -19$ arise because Lyα REWs greater than our quoted REW$_{min}$ are required to render the Lyα flux large enough (i.e. $L_\alpha \geqslant L_{\alpha,min}$, see Table 2) to be detected from fainter UV magnitudes. For example, in order for an object to be detected in Lyα from an $M_{UV} = -18.5$ galaxy, we need REW> 100 Å, and these objects are significantly rarer. Note that the 'sharpness' of the break increases towards lower redshift. This is because the scale-length of the REW-PDF increases with redshift (see Fig 1), and objects with REW> 100 Å are rarer at lower redshift.

The agreement between our model and the data is excellent at $z = 3.1$ (*left panel*, note that this is not a fit), and reasonable at $z = 3.7$ (*central panels*). In the $z = 3.7$ case, the observed UV-LF suffers from incompleteness at $M_{UV} > -20.0$, and so our formalism therefore overpredicts only the brightest UV point. Our best-fit $z = 5.7$ model clearly underpredicts the LAE UV-LF at $z = 5.7$ (*right panel*) at $-20 < M_{UV} < -21.4$. The reason for this is not clear. It is possibly related to the fact that we overproduce the number of large REW (REW $\gtrsim 200$ Å) systems (see below), although this discrepancy in the REW distribution is quite small.

3.3 The Lyα Equivalent Width Distribution

We also use our formalism to predict the REW distribution (derived in Appendix B) for our best-fit model

$$P(\mathrm{REW}, z) = \mathcal{N} \int_{L_{\alpha,\mathrm{min}}}^{L_{\alpha,\mathrm{max}}} P(\mathrm{REW}|M_{\mathrm{UV,c}}, z)\phi(M_{\mathrm{UV,c}}, z) d\log_{10} L_\alpha, \quad (5)$$

where $\mathcal{N}$ denotes a normalization constant, $\phi(M_{\mathrm{uv}}, z)$ again denotes the LBG UV luminosity function (introduced in § 2), and $P(\mathrm{REW}|M_{\mathrm{UV,c}}, z)$ denotes the Lyα-REW PDF that is observed for LBGs. The relation between Lyα luminosity, UV continuum flux density, and REW uniquely determines the absolute UV magnitude $M_{\mathrm{UV,c}}$ at fixed L_α and REW. This equation states that at a given Lyα luminosity, the probability of observing a galaxy with Lyα REW is the sum of all possible M_{UV}, weighted by their number density.

Figure 3 shows our model equivalent width PDF (*black thick solid lines*). The *red filled squares* show the observed REW PDF for all photometrically selected LAEs (also shown as the *black histograms* in Fig 23 of Ouchi et al. 2008). The *blue dashed histograms* show the observed REW distribution of spectroscopically confirmed LAEs. At $z = 3.1$ (*left panel*) our model underpredicts the observed number of drop-out galaxies with REW> 175 Å. The agreement between our model and the data at $z = 3.7$ is excellent. As eluded to previously, our model slightly overpredicts the number of large REW systems (REW> 200 Å) at $z = 5.7$, which partially explains why we underpredict the observed UV-LF of LAEs at $z = 5.7$.

4 DISCUSSION

In the previous section we showed that the observed REW distribution of LAEs can be reproduced well out to REW$=200$ Å using sharp cuts in REW and Lyα luminosity among the drop-out population. However our empirical procedure leads to LAE luminosity functions (both UV and Lyα) that are overpredicted by a factor of $1/F \sim 2.5$. As already noted, the difference of F from unity indicates that simple selection cuts in luminosity and REW do not adequately represent the LAE selection. The goal of this discussion is to explore the observational biases and model assumptions that may cause F to be less than 1.

4.1 Discussion of Observational Biases

Firstly, we note that using the drop-out galaxy population to constrain the number density of star forming galaxies as a function of their UV and Lyα luminosity, does not miss the small fraction of 'red' star forming galaxies (e.g. those with UV slopes $\beta \gtrsim -0.5$, Bouwens et al. 2009), since the drop-out galaxy luminosity functions used in this paper have been corrected for this bias (see Bouwens et al. 2009). Secondly, narrowband surveys can pick up galaxies such as ULIRGs which do not make it into drop-out surveys (Nilsson & Møller 2011). However, the ULIRG fraction among LAEs drops dramatically to $\lesssim 10\%$ at $z > 2.5$ (Nilsson & Møller 2011), and this is unlikely to be a significant effect. A hypothetical population of LAEs whose Lyα

emission is powered predominantly by gravitational heating (as in e.g. Birnboim & Dekel 2003, Dijkstra 2009, Dayal et al. 2010), would also contribute to LAE samples. However these known potential observational biases would enhance the true number density of LAEs, and thus lead to a value of $F > 1$.

Ouchi et al. (2008) discuss possible explanations why $F > 1$. Some of these possibilities could also result in $F < 1$. These include: (*i*) Systematic uncertainties in drop-out galaxy luminosity functions, based the observed scatter in the $z = 6$ drop-out LFs obtained by different groups. (*ii*) The fact that drop-out LFs at a particular redshift are measured over a much broader redshift interval ($\Delta z \sim 1$) than is probed by narrowband surveys. These differences may introduce extra uncertainties when comparing LAE and drop-out galaxy populations.

We have investigated whether our results are dominated by observations at a particular redshift, and repeated our analysis based on the LAE luminosity function in individual redshift bins (while fixing $\frac{d\mathrm{REW}_{\mathrm{crit}}}{dz} = 6$ Å). We find that $F = 0.34^{+0.46}_{-0.17}$ at $z = 3.1$, $F = 0.44^{+0.48}_{-0.21}$ at $z = 3.7$ and $F = 0.52^{+0.48}_{-0.23}$ at $z = 5.7$, where the uncertainty on F is dominated by cosmic variance. Thus, our result is not dominated by any redshift bin. The systematic effect that causes $F < 1$ appears to operate at all redshifts.

4.2 Discussion of Model Assumptions

In this section we discuss the effects of different assumptions on our results, with particular focus on the conclusion that $F < 1$.

Assumption 1. In our fiducial model we assume that the fitting formula for REW (Eq 3) applies only in the observed range of UV magnitudes, and freeze its evolution for $M_{\mathrm{UV}} > -19.0$. On the other hand, Stark et al. (2010) find that the observed evolution in the REW-PDF continues down to $M_{\mathrm{UV}} = -18.5$ (see the *left panel* of their Fig 13), albeit with large uncertainties. Had we extrapolated our fitting function down to fainter UV magnitudes, then we would have allowed more UV-faint, large REW galaxies into our sample. However, if we include these UV-faint sources, then we would push our constraints on F to lower values, which would rule out $F = 1$ at greater significance. Conversely, the uncertainties on the REW-PDF are large at $M_{\mathrm{UV}} \geqslant -19.0$. If we had frozen the evolution of the REW-PDF at $M_{\mathrm{UV}} \geqslant -19.25$, then we would have found a larger value of F, especially when combined with a truncation of the REW-PDF at REW$\geqslant 150$ Å (see below).

Assumption 2. In our fiducial model we chose $x_{\mathrm{max}} = \mathrm{REW}_{\mathrm{max}} = 300$ Å to be the maximum possible Lyα REW. This value is close to the largest REW in the sample of Ouchi et al. (2008). Theoretically, the Lyα REW can reach $\sim 1500 - 3000$ Å for metal free galaxies forming stars with a top-heavy IMF (Schaerer 2003, Johnson et al. 2009, Raiter et al. 2010), or cooling clouds (Dijkstra, 2009), and could be boosted to even larger values if dust preferentially suppresses the UV continuum (Neufeld 1991; Hansen & Oh 2006). Adopting larger values for REW$_{\mathrm{max}}$ would boost the overall Lyα emissivity of star forming galaxies, which would again reduce our best-fit values for F.

We note that there is limited data to support the assumed exponential form of the REW-PDF at REW $\gtrsim 150$ Å.

Indeed, among the ~ 800 LBGs in the sample of Shapley et al. (2003), only 4 (1) have REW$\geqslant 150$ (175) Å, so that the observed REW-PDF among LBGs is very uncertain at these values. If we truncate the REW-PDF at REW$_{max} = 150$ Å, then we find $F = 0.64^{+0.20}_{-0.12}$, and $F = 1$ is only ruled out at $\sim 89\%$ CL. If we further combine this with 'freezing' the evolution of the REW-PDF at $M_{UV} \geqslant -19.25$, then we find $F = 0.70^{+0.23}_{-0.14}$, and $F = 1$ is only ruled out at $\sim 77\%$ CL. While these modified assumptions do not fully resolve the issue, they do illustrate that our finding of $F \ll 1$ depends on the uncertain REW-PDF at REW $\gtrsim 150$ Å and faint M_{UV}. We note that if we assume REW$_{max} = 150$ Å, then our model does not produce LAEs with REW$\geqslant 150 Å$, although these objects *are* observed. However, considering just LAEs that have been confirmed spectroscopically, this appears to be a significant problem only at $z = 5.7$, where the uncertainties on measured REWs are large (see Table 2 of Ouchi et al. 2008).

Assumption 3. In our fiducial model we assumed that $\beta = -1.7$. Stark et al. (2010) found that $\beta = -1.6$ for drop out galaxies with REW< 50 Å, and $\beta = -2.0$ when REW$\geqslant 50$ Å for $-21.5 < M_{UV} < -20.5$. For fainter galaxies with REW< 50 Å, β approaches -2.0. Our choice for β may be slightly too high (also see Bouwens et al. 2009, 2010b). However, if we decrease β then we *increase* the total Lyα flux for a fixed REW and M_{UV}, and thus the overall Lyα emissivity of the drop-out galaxy population. Decreasing β would therefore again lower our overall best-fit value for F.

4.3   Comparison to Previous Work

Our study bares similarities to that of Malhotra & Rhoads (2002). These authors also compared observations with 'predicted' LAE number counts and REW distributions, which they obtained by combining existing constraints on the faint-end of the $z \sim 4$ drop-out galaxy luminosity function with a theoretical model for the Lyα REW-distribution. However, modeling the observed equivalent width of the Lyα emission line is a complicated task which depends on detailed radiative transfer of Lyα photons through both ISM and IGM. Our calculations completely circumvent this complication by utilizing empirical distributions, which represents an important improvement. In agreement with our findings, the study of Malhotra & Rhoads (2002) also overpredicted the number density of LAEs. Their offset was by an even larger factor of $\sim 6 - 12$, implying that only $\sim 7 - 15\%$ of all LBGs need to be LAEs. However our formalism already includes the observation that only a fraction of the drop-out population has strong enough Lyα emission to qualify as a LAE. Thus the concept of separate galaxy populations cannot be invoked to explain the offset ($F \neq 1$).

5   EXTRAPOLATING TO REDSHIFTS $Z \sim 7 - 9$

There are existing constraints on the LBG luminosity functions at $z > 6$. It is therefore interesting to take our best-fit model and predict the expected number density of LAEs at redshifts beyond those currently observed. Before doing so, we first point out that extrapolating the REW-PDF of our best-fit model to $z > 6$ leads to inconsistencies with some available data.
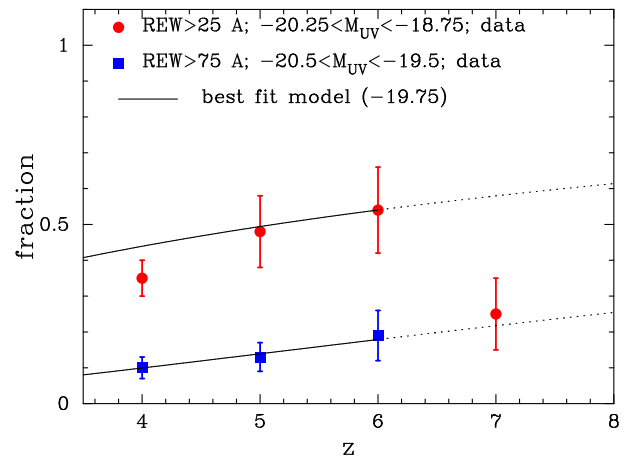

Figure 4. The fraction of drop-out galaxies with Lyα emission lines with REW$> x$ as a function of redshift. *Blue filled squares* show the data from Stark et al. (2010) for galaxies with $-20.5 < M_{UV} < -19.5$ and $x = 75$ Å, while *red filled circles* show the data from Stark et al. (2010); Pentericci et al. (2011); Schenker et al. (2011); Pentericci et al. (2011) compiled by Ono et al. (2011) for $-20.25 < M_{UV} < -18.75$ and $x = 25$ Å. The *solid lines* shows our best fit model (this model was fitted to the Lyα luminosity functions, not this data), which provides and excellent fit to the data for our purposes (see text). The *dotted lines* show our best-fit model extrapolated to $z \geqslant 6$. The observed fraction at $z = 7$ falls well below this extrapolation.

The observed fraction of drop-out galaxies having Lyα emission lines of REW$\geqslant x$ has been measured as a function of redshift out to $z \sim 7$ for galaxies with $-20.5 < M_{UV} < -19.5$ for $x = 75$ Å (Stark et al. 2010), and for galaxies with $-20.25 < M_{UV} < -18.75$ for $x = 25$ Å (Pentericci et al. 2011; Schenker et al. 2011; Ono et al. 2011, also see Vanzella et al. 2011). In Figure 4, we compare the data from Stark et al. (2010, *blue filled squares*), and the data compiled by Ono et al. (2011, *red filled circles*) with our best-fit model of § 3 (*solid lines*). Our best fit-model slightly overpredicts (by a factor of ~ 1.2) the fraction of drop-out galaxies for which REW$\geqslant 25$ Å at $z \leqslant 4$. However, at these redshifts REW$_{min} \geqslant 44$ Å, and our results depend weakly on this discrepancy. For our purposes, the agreement between our model and the data is excellent out to $z \sim 6$. We stress that this best-fit model was fitted to the Lyα luminosity functions, and not these particular data points. This indicates that our model reproduces the observed redshift *evolution* of LAEs well, despite the fact that the overall predicted number density is off by a factor of F. However observations indicate that a sudden drop occurs in the 'LAE fraction' at $z > 6$, and the linear extrapolation of our model does not reproduce this evolution.

To remain consistent with the observed drop in the 'LAE fraction', we replace the term REW$_{c,0} + \frac{d\text{REW}_c}{dz}\Delta z$ (yielding REW$_{c,7} = 43$ Å), in our best fit model with REW$_{c,7} = 8$ Å . This ensures that we reproduce the observed drop in the LAE fraction. Otherwise, we take the Schechter function parameters given in Table 1, and the model parameters from our best-fit model. In the *left panel* of Figure 5 the *red solid line* shows the predicted number density of LAEs (in cMpc^{-3} log$^{-1}L_\alpha$) at $z = 7$, where we further assumed REW$_{min} = 27$ Å(to facilitate the comparison with the $z = 5.7$ data by Ouchi et al. 2008). Our model pre-

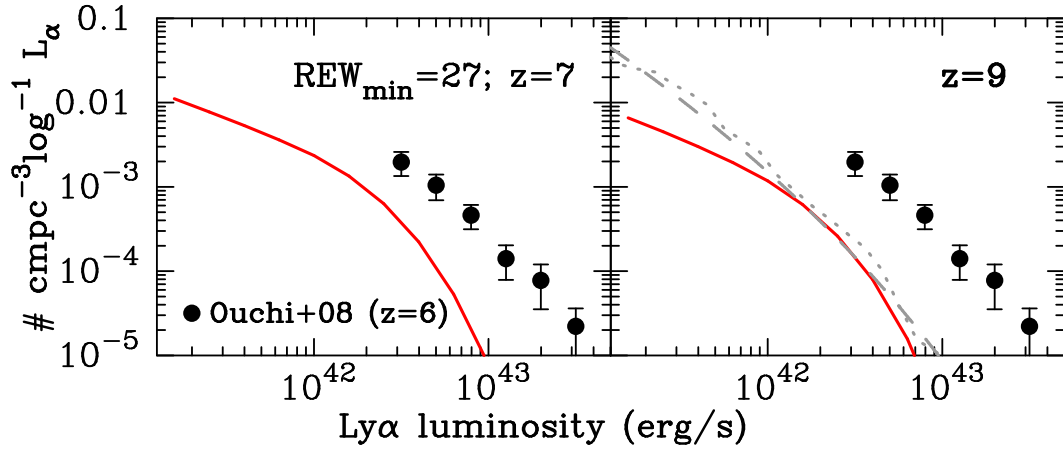**Figure 5.** *Left Panel:* Predicted number density of LAEs (in cMpc^{-3} log^{-1}L_α) at $z = 7$ (*solid red line*). *Right panel:* Same as the *left panel*, but at $z = 9$. Within the range of luminosities that will likely be probed by future surveys, $L_\alpha \sim 10^{41} - 10^{43}$ erg s^{-1}, the agreement between previous model predictions (here *dashed line* is the GALFORM model from Nilsson et al. 2007, and the *dotted line* is the model of Dijkstra et al. 2007a) and those inferred from the z=9 LBG population is quite good (see text).

dicts the cumulative number density of LAEs brighter than $L_\alpha = 10^{43}$ erg s^{-1} to be $n(L_\alpha > 10^{43}$ erg/s) $\sim 10^{-6}$ cMpc^{-3}, which is below the observational constraints by Ota et al. (2010). However the observational constraints are uncertain given that their observed cumulative luminosity function is derived from only three objects. Our predicted luminosity functions are in turn affected by uncertainties in our model parameter vector **P**. For example, taking REW$_{c,7}$ = 15 Å– which gives a Lyα fraction among $z \sim 7$ drop-out galaxies of 35%– results in $n(L_\alpha > 10^{43}$ erg/s) $\sim 5 \times 10^{-6}$ cMpc^{-3}, which is within $1 - \sigma$ of the best-fit value derived by Ota et al. (2010). Note that similar uncertainties will apply to any theoretical model, as these are likely to be –just like our parameter vector **P**–calibrated by lower-redshift data.

The *right panel* of Figure 5 shows our predictions for redshift $z = 9$. We assumed $M^*_{\rm UV} = -19.1$, which we obtained by extrapolating the observed redshift evolution at lower redshift ($z \leqslant 6$) $M^*_{\rm UV} = -21.02 + 0.36(z - 3.8)$ (Bouwens et al. 2008), and we assumed that REW$_{c,9}$ =REW$_{c,7}$. This extrapolated value is consistent with the derived lower limit $M^*_{\rm UV} \gtrsim -19.6$ derived by Bouwens et al. (2008) based on the absence in J-dropouts in the Hubble Ultra Deep Field (see Oesch et al. 2011 for constraints on the $z = 10$ drop-out galaxy luminosity function using deeper and wider WFC3-IR data). For completeness, we have overplotted some theoretical predictions for the number density of LAEs at $z = 9$. The *dotted line* shows the predicted number density of LAEs at $z = 8.8$ by Nilsson et al. (2007) who used the semi-analytic model GALFORM (Cole et al. 2000). The *dashed line* was obtained from a simpler model in which some fraction f_* of all baryons is converted into stars over a timescale $\epsilon_{\rm DC}t_{\rm hub}$ (Dijkstra et al. 2007a). These simpler models easily reproduce the observed number density of LAEs at $z \geqslant 5.7$, and have been used frequently in the recent literature. The theoretical predictions also agree well with each other, which is probably because the models are calibrated by the same lower redshift data. The theoretically predicted luminosity functions decrease more steeply than those obtained from the LBG population. However, given the present-day uncertainties on the $z = 9$ LBG luminosity function, it is not clear how significant

this difference is. For example, a steeper faint end slope of the $z = 9$ luminosity function would would reduce the discrepancy. Observations indicate that this faint end slope may indeed become steeper at higher redshifts (Bouwens et al. 2011, also see Jaacks et al. 2011).

6 CONCLUSIONS

In this paper we have investigated the implications of the assumption often used in theoretical modelling that the LAEs are selected using cuts in REW and luminosity. These cuts are only coarse approximations to the detailed criteria that are employed in observational studies. To quantify the importance of the approximation, we investigated whether we can reproduce LAE data if we define LAEs using a (redshift-dependent) Lyα luminosity and EW threshold, and a empirical model for the number density of star forming galaxies as a function of their UV and Lyα luminosity. We constructed this model by combining observed luminosity functions of drop-out galaxies, with the observed rest-frame equivalent width (REW) probability distribution function (PDF) of drop-out galaxies at $z = 3 - 7$, and 'predicted' the resulting Lyα luminosity function at $z = 3.1$, $z = 3.7$ and $z = 5.7$. We also use our formalism to predict the UV LF of Ly-α emitters, and the EW observed distribution of Ly-α emitters.

As part of our analysis we demonstrate that the observed REW-PDF of $z = 3$ LBGs is well described by an exponential function at REW$\geqslant$ 0, i.e. P(REW) $\propto$ exp[$-$REW/REW$_c$($M_{\rm UV}$)]. The scale length depends on absolute UV-magnitude, and we use recent data from Stark et al. (2010, 2011) to constrain this dependence. Using this empirical distribution of REW in LBGs, we find that we can reproduce the observed REW distribution for LAEs quite well out to REW$\sim$ 200 Å. However, in order to reproduce the LAE luminosity functions, we find that we must re-scale the predicted luminosity functions downward by a factor of $F = 0.43^{+0.14}_{-0.07}$. Formally, a value of $F = 1$, which is expected if the simple REW and luminosity cuts are accurate, is ruled out at $\sim$ 95%. We found that this discrepancy can be reduced if we truncate the Lyα REW-PDF at REW$\geqslant$ 150

Å, and 'freeze' its evolution at $M_{\rm UV} \gtrsim -19.25$. The sample of Shapley et al (2003) only contains 4 drop-out galaxies (out of 797) with REW$\geqslant 150$ Å, and observationally the REW-PDF is constrained very poorly at these large values for REW. For this truncated REW-PDF, which stops evolving at $M_{\rm UV} \gtrsim -19.25$, we find $F = 0.70^{+0.23}_{-0.15}$, and $F = 1$ is ruled out only at $\sim 77\%$.

On the other hand, we found that the overall redshift evolution of the LAEs was reproduced very well by our empirical model. Encouraged by this result, we combine the best-fit model in our formalism with recent observed constraints of the 'LAE fraction' and predict number densities of LAEs at $z = 7$ and $z = 9$. Current measurements of the LBG luminosity functions translate to Lyα luminosity functions that are consistent with observed number counts of LAEs at $z = 7$, but which are still very uncertain. Nevertheless the UV LF of LBGs can be used to provide empirical guidance for future surveys aiming to discover Ly-α galaxies at the highest redshifts.

We conclude that modeling LAEs with simple REW and luminosity cuts can lead to (significant) changes to the predicted number density of LAEs. Theorists will therefore need to make more careful account of observational selection in order to produce reliable models of the observed population. This will have to include application of the proper filter transmission curves to generate mock data from the models, *and* then correct for these filter transmission curves following the same procedures as followed by the observers whose data one tries to reproduce. We are attempting to address these issues in more detail in on-going work. Furthermore, our work has shown that to in order to address this issue in more detail, it will be important to reduce the observational uncertainties associated with the REW-PDF of drop-out galaxies at large REW and/or faint $M_{\rm UV}$.

REFERENCES

Atek, H., Schaerer, D., & Kunth, D. 2009, A&A, 502, 791
Barnes, L. A., Haehnelt, M. G., Tescari, E., & Viel, M. 2011, arXiv:1101.3319
Birnboim, Y., & Dekel, A. 2003, MNRAS, 345, 349
Blanc, G. A., et al. 2011, submitted to ApJ, arXiv:1011.0430
Bouwens, R. J., Illingworth, G. D., Blakeslee, J. P., & Franx, M. 2006, ApJ, 653, 53
Bouwens, R. J., Illingworth, G. D., Franx, M., & Ford, H. 2007, ApJ, 670, 928
Bouwens, R. J., Illingworth, G. D., Franx, M., & Ford, H. 2008, ApJ, 686, 230
Bouwens, R. J., et al. 2009, ApJ, 705, 936
Bouwens, R. J., et al. 2010a, ApJL, 709, L133
Bouwens, R. J., et al. 2010b, ApJL, 708, L69
Bouwens, R. J., et al. 2011, arXiv:1105.2038
Bunker, A. J., et al. 2010, MNRAS, 1378
Clément, B., et al. 2011, arXiv:1105.4235
Cole, S., Lacey, C. G., Baugh, C. M., & Frenk, C. S. 2000, MNRAS, 319, 168
Cowan, G. 1997, Statistical data analysis. Publisher: Oxford: Clarendon Press, 1998 Series: Oxford science publications. ISBN: 0198501560,
Dawson, S., Rhoads, J. E., Malhotra, S., Stern, D., Wang, J., Dey, A., Spinrad, H., & Jannuzi, B. T. 2007, ApJ, 671, 1227
Dayal, P., Ferrara, A., & Saro, A. 2010, MNRAS, 402, 1449
Dayal, P., Maselli, A., & Ferrara, A. 2011, MNRAS, 410, 830
Dessauges-Zavadsky, M., D'Odorico, S., Schaerer, D., Modigliani, A., Tapken, C., & Vernet, J. 2010, A&A, 510, A26
Dijkstra, M., Wyithe, J. S. B., & Haiman, Z. 2007a, MNRAS, 379, 253
Dijkstra, M., Lidz, A., & Wyithe, J. S. B. 2007b, MNRAS, 377, 1175
Dijkstra, M. 2009, ApJ, 690, 82
Dijkstra, M., & Westra, E. 2010, MNRAS, 401, 2343
Dijkstra, M., & Wyithe, J. S. B. 2010, MNRAS, 408, 352
Dijkstra, M., Mesinger, A., & Wyithe, J. S. B. 2011, MNRAS, 414, 2139
Fernandez, E. R., & Komatsu, E. 2008, MNRAS, 384, 1363
Finkelstein, S. L., Papovich, C., Giavalisco, M., Reddy, N. A., Ferguson, H. C., Koekemoer, A. M., & Dickinson, M. 2010, ApJ, 719, 1250
Finkelstein, S. L., Cohen, S. H., Moustakas, J., Malhotra, S., Rhoads, J. E., & Papovich, C. , submitted to ApJ, arXiv:1012.4010
Forero-Romero, J. E., Yepes, G., Gottlöber, S., Knollmann, S. R., Cuesta, A. J., & Prada, F. 2011, MNRAS, 981
Gawiser, E., et al. 2007, ApJ, 671, 278
Gronwall, C., et al. 2007, ApJ, 667, 79
Guaita, L., et al. 2010, ApJ, 714, 255
Haiman, Z., & Spaans, M. 1999, ApJ, 518, 138
Hansen, M., & Oh, S. P. 2006, MNRAS, 367, 979
Hayes, M., Schaerer, D., Östlin, G., Mas-Hesse, J. M., Atek, H., & Kunth, D. 2011, ApJ, 730, 8
Hibon, P., et al. 2010, A&A, 515, A97
Hopkins, A. M., & Beacom, J. F. 2006, ApJ, 651, 142
Hu, E. M., Cowie, L. L., & McMahon, R. G. 1998, ApJL, 502, L99
Hu, E. M., Cowie, L. L., McMahon, R. G., Capak, P., Iwamuro, F., Kneib, J.-P., Maihara, T., & Motohara, K. 2002, ApJL, 568, L75
Hu, E. M., Cowie, L. L., Barger, A. J., Capak, P., Kakazu, Y., & Trouille, L. 2010, ApJ, 725, 394
Iliev, I. T., Shapiro, P. R., McDonald, P., Mellema, G., & Pen, U.-L. 2008, MNRAS, 391, 63
Iye, M., et al. 2006, *Nature*, 443, 186
Jaacks, J., Choi, J.-H., & Nagamine, K. 2011, arXiv:1104.2345
Johnson, J. L., Greif, T. H., Bromm, V., Klessen, R. S., & Ippolito, J. 2009, MNRAS, 399, 37
Kashikawa, N., et al. 2006, ApJ, 648, 7
Kashikawa, N., et al. 2011, ApJ, 734, 119
Kobayashi, M. A. R., Totani, T., & Nagashima, M. 2010,

ApJ, 708, 1119

Komatsu, E., et al. 2009, ApJS, 180, 330

Kovač, K., Somerville, R. S., Rhoads, J. E., Malhotra, S., & Wang, J. 2007, ApJ, 668, 15

Laursen, P., Sommer-Larsen, J., & Andersen, A. C. 2009, ApJ, 704, 1640

Laursen, P., Sommer-Larsen, J., & Razoumov, A. O. 2011, ApJ, 728, 52

Le Delliou, M., Lacey, C. G., Baugh, C. M., & Morris, S. L. 2006, MNRAS, 365, 712

Lehnert, M. D., et al. 2010, *Nature*, 467, 940

Malhotra, S., & Rhoads, J. E. 2002, ApJL, 565, L71

Malhotra, S., & Rhoads, J. E. 2006, ApJL, 647, L95

Mao, J., Lapi, A., Granato, G. L., de Zotti, G., & Danese, L. 2007, ApJ, 667, 655

McQuinn, M., Hernquist, L., Zaldarriaga, M., & Dutta, S. 2007, MNRAS, 381, 75

Moster, B. P., Somerville, R. S., Newman, J. A., & Rix, H.-W. 2011, ApJ, 731, 113

Muñoz, J. A., Trac, H., & Loeb, A. 2010, MNRAS, 405, 2001

Nagamine, K., Ouchi, M., Springel, V., & Hernquist, L. 2010, PASJ, 62, 1455

Neufeld, D. A. 1991, ApJL, 370, L85

Nilsson, K. K., Orsi, A., Lacey, C. G., Baugh, C. M., & Thommes, E. 2007, A&A, 474, 385

Nilsson, K. K., Möller-Nilsson, O., Møller, P., Fynbo, J. P. U., & Shapley, A. E. 2009, MNRAS, 1308

Nilsson, K. K., & Møller, P. 2011, A&A, 527, L7

Oesch, P. A., et al. 2011, arXiv:1105.2297

Ono, Y., et al. 2011, arXiv:1107.3159

Ota, K., et al. 2008, ApJ, 677, 12

Ota, K., et al. 2010, ApJ, 722, 803

Ouchi M., et al., 2008, ApJS, 176, 301

Ouchi, M., et al. 2010, ApJ, 723, 869

Paltani, S., et al. 2007, A&A, 463, 873

Partridge, R. B., & Peebles, P. J. E. 1967, ApJ, 147, 868

Pentericci, L., et al. 2011, arXiv:1107.1376

Raiter, A., Schaerer, D., & Fosbury, R. A. E. 2010, A&A, 523, A64

Rauch, M., et al. 2008, ApJ, 681, 856

Reddy, N. A., & Steidel, C. C. 2009, ApJ, 692, 778

Rhoads, J. E., Malhotra, S., Dey, A., Stern, D., Spinrad, H., & Jannuzi, B. T. 2000, ApJL, 545, L85

Robertson, B. E., Ellis, R. S., Dunlop, J. S., McLure, R. J., & Stark, D. P. 2010, *Nature*, 468, 49

Santos, M. R. 2004, MNRAS, 349, 1137

Schaerer, D., & Verhamme, A. 2008, A&A, 480, 369

Schenker, M. A., Stark, D. P, Ellis, R. S., Robertson, B. E., Dunlop, J. S., McLure, R. J., Kneib, J. -., & Richard, J. 2011, arXiv:1107.1261

Shapley, A. E., Steidel, C. C., Pettini, M., & Adelberger, K. L. 2003, ApJ, 588, 65

Shimasaku, K., et al. 2003, ApJ, 586, L111

Shimasaku K., et al., 2006, PASJ, 58, 313

Shimizu, I., Yoshida, N., & Okamoto, T. 2011, arXiv:1102.1509

Somerville, R. S., Lee, K., Ferguson, H. C., Gardner, J. P., Moustakas, L. A., & Giavalisco, M. 2004, ApJL, 600, L171

Stanway, E. R., McMahon, R. G., & Bunker, A. J. 2005, MNRAS, 359, 1184
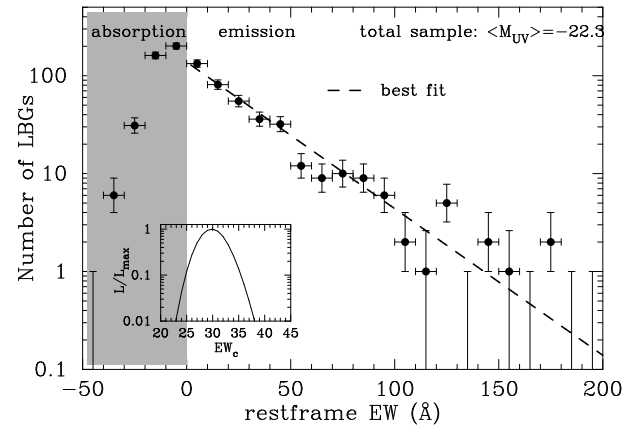
Stanway, E. R., et al. 2007, MNRAS, 376, 727

Figure A1. The observed Lyα rest frame equivalent width (REW) distribution of ∼ 800 $z \sim 3$ LBGs of the sample of Shapley et al. (2003) is shown as the *black histogram*. This sample had a median $M_{\rm UV} = -22.3$. This figure shows that the observed REW-PDF can be described well by an exponential function.

Stark, D. P., Ellis, R. S., Chiu, K., Ouchi, M., & Bunker, A. 2010a, MNRAS, 408, 1628

Stark, D. P., Ellis, R. S., & Ouchi, M. 2011, ApJL, 728, L2

Steidel, C. C., Giavalisco, M., Pettini, M., Dickinson, M., & Adelberger, K. L. 1996, ApJL, 462, L17

Steidel, C. C., Bogosavljević, M., Shapley, A. E., Kollmeier, J. A., Reddy, N. A., Erb, D. K., & Pettini, M. 2011, arXiv:1101.2204

Tilvi, V., et al. 2010, ApJ, 721, 1853

Vanzella, E., et al. 2011, ApJL, 730, L35

Willis, J. P., Courbin, F., Kneib, J.-P., & Minniti, D. 2008, MNRAS, 384, 1039

Yan, H.-J., Windhorst, R. A., Hathi, N. P., Cohen, S. H., Ryan, R. E., O'Connell, R. W., & McCarthy, P. J. 2010, Research in Astronomy and Astrophysics, 10, 867

Zheng, Z., Cen, R., Trac, H., & Miralda-Escudé, J. 2010a, ApJ, 716, 574

Zheng, Z., Cen, R., Trac, H., & Miralda-Escude, J. 2010b, submitted to ApJ

APPENDIX A: ACCURACY OF FITTING FORMULA FOR OBSERVED EW-PDF

A1 Fiducial REW-PDF Parameterization

In our paper we approximate the observed Lyα REW distribution using the functional form given by Eq 3. This functional form is motivated by several factors.

• The observed REW-PDF of $z = 3$ LBGs is well described by an exponential function. This is illustrated in Fig A1, where the *histogram* shows the observed number of LBGs as a function of Lyα REW (Shapley et al. 2003). This sample had a median $M_{\rm UV} = -22.3$. The *inset* of this Figure shows that the best-fit scale-length associated with this exponential distribution is $REW_{\rm c} \sim 29$ Å, for which the function is overplotted as the *dotted line*.

• The scalelength $REW_{\rm c}$ is observed to be a function of absolute UV magnitude, $M_{\rm UV}$ (Shapley et al. 2003). This is illustrated in Figures A2 and A3, where show the REW-PDF for subsamples of the brightest ∼ 400 LBGs (Fig A2), and
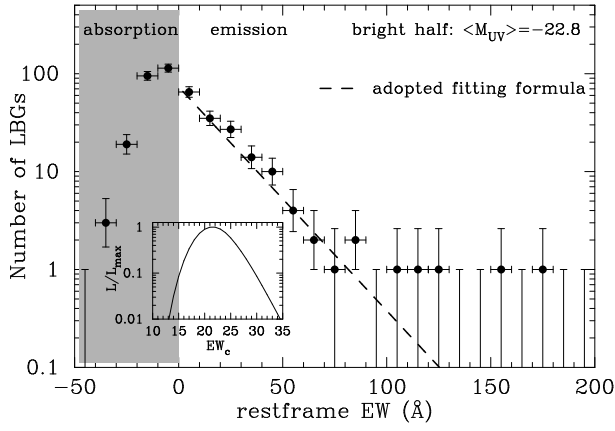
Figure A2. The observed Lyα rest frame equivalent width (REW) distribution of the brightest 399 $z = 3$ LBGs of the sample of Shapley et al. (2003) is shown as the *black histogram*. This sample had a median $M_{UV} = -22.8$, and is labeled the 'bright' sample. The *dashed line* shows our adopted fitting formula (Eq 3). Our fitting formula provides a decent fit to the data.
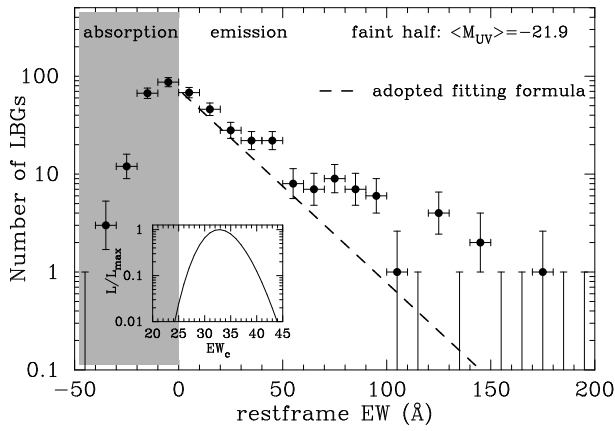

Figure A3. Same as Figure A2, but for the faintest 398 LBGs. Our fitting function now underpredicts the number of large EW systems significantly. This is because our fitting formula adopts $REW_c = 22$ Å, while the best fit $REW_c = 33$ Å. Our fitting formula *underpredicts* the number of large EW systems. Applying a correction for this would lower our required values for F (see text), strengthening the conclusions of this work.

of the faintest 400 LBGs (Fig A3). The *thick dashed lines* show our adopted fitting formula. The figure shows that our fitting formula provides a good fit to the 'bright' sample, but significantly underpredicts the number of large EW systems in the 'faint' sample (Fig A3). This is because our fitting formula adopts $REW_c = 22$ Å, while the best fit to this subsample is $REW_c = 33$ Å (see the *inset*). On the other hand this choice is required in order to be consistent with data at fainter UV magnitudes (see below). We stress that our fitting formula *underpredicts* the number of large EW systems at faint UV magnitudes. Applying the correction would lower our required values for F (see text), strengthening the conclusions of this work.
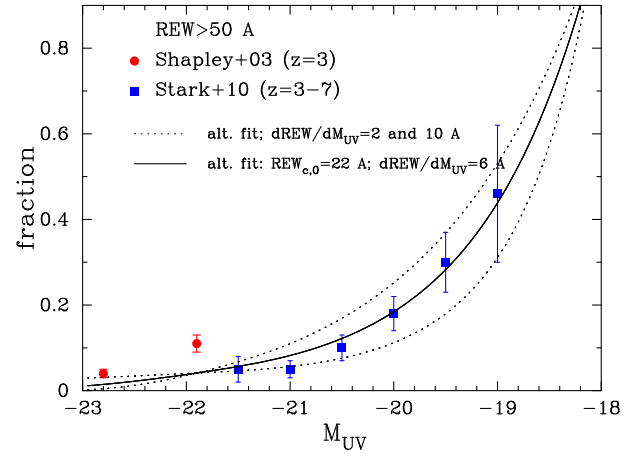

Figure A4. This Figure shows the fraction of drop-out galaxies with a Lyα REW > 50 Å, as a function of M_{UV}. The *red circles* represent the $z = 3$ data of Shapley et al. (2003, also shown in Fig A2 and Fig A3). The *blue squares* represent data from Stark et al. (2010) from a Keck spectroscopic survey of $z = 3 - 7$ drop-out galaxies. The *black solid line* shows our fitting function. The *black dotted lines* show our fitting function when we increase or decrease the parameter $\frac{dREW}{dM}$ by 4 Å. Our fitting function is clearly consistent with the data (see text).

• We choose the normalization[5] factor such that all drop-out galaxies have $-a_1 \leqslant REW \leqslant REW_{max}$. While there are drop-out galaxies with smaller REW, this choice automatically results in a fraction of drop-out galaxies with Lyα *in emission* (i.e. REW > 0) that increases with M_{UV}, as observed in the sample of Shapley et al (2003). This choice for the normalization constraint allows us to describe the M_{UV}–dependence of the observed shape and normalization of the Lyα REW PDF at REW> 0 with one single parameter, namely REW_c (we keep a_1 constant within this range). However, as we show next this single parameter description breaks down at fainter ($M_{UV} \gtrsim -21.5$) magnitudes.

• Stark et al. (2010) found that the REW-PDF is sensitive to M_{UV}. This dependance is relatively weak in the range $-22.0 < M_{UV} < -20.5$, but strong from $-20.5 < M_{UV} < -18.5$. This is shown in Fig A4, where we compare the observed fraction of drop-out galaxies with REW> 50 Å as a function of M_{UV} to our fit. The *red squares* show the data presented by Shapley et al. (2003), while the *blue circles* show the data presented by Stark et al. (2010). The *solid curve* represents our adopted fitting function. We match the rapid evolution at $M_{UV} > -20.5$ by decreasing a_1 as described in the paper. The *dotted curves* show the model when we increase or decrease the parameter $\frac{dREW}{dM}$ by 4 Å. Note that the data point at $M_{UV} = -21.9$ lies a few σ above our fitting function, because this data point lies significantly above the data at $-21.5 \leqslant M_{UV} \leqslant -21.0$. Forcing better agreement with this data point therefore automatically results in worse agreement with the data at fainter UV magnitudes. This is why our best-fit model does not provide the best fit to the data shown in Figure A3.

---

[5] This factor is given by $\mathcal{N} = \left[\exp\left(\frac{-a_1}{REW_c(M_{UV})}\right) - \exp\left(\frac{REW_{max}}{REW_c(M_{UV})}\right)\right]/REW_c(M_{UV})$.
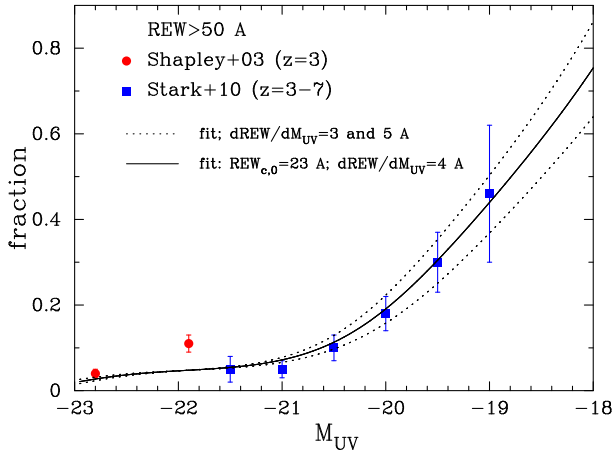
Figure A5. Same as Figure A4, but for our alternative parametrization of the REW-PDF (see text).

A2 Alternative Parametrization of the EW-PDF

To make sure our results do not depend on our chosen functional form, we also study an alternative parametrization of the Lyα REW PDF. In this model, parametrize the observed shape and normalization of the Lyα REW PDF at REW> 0 at all $M_{\rm UV}$ with a single parameter (REW$_{\rm c}$). To capture the observed evolution of the REW-PDF with $M_{\rm UV}$ (weak in the range $-22.0 < M_{\rm UV} < -20.5$, and strong from $-20.5 < M_{\rm UV} < -18.5$), we add a cubic term $(\Delta M)^3$ into the expression for REW$_{\rm c}(M_{\rm UV})$. Specifically, we keep the parameter $a_1 = -20$ Å fixed at all $M_{\rm UV}$, and REW$_c(M_{\rm UV}) =$ REW$_{\rm c,0} + b(\Delta M + [\Delta M]^3) + \frac{d{\rm REW}_c}{dz}\Delta z$. The data is well described by REW$_{\rm c,0} = 23\pm2$ Å and $b = 4.4\pm1$Å (see Figure A5).

We have repeated our analysis by fitting the observed Lyα luminosity function for this alternative model. In our standard model (see § 4.2) we keep the evolution of the REW-PDF constant at $M_{\rm UV} \geqslant -19.0$. The results of this analysis are presented in Figures A6, which shows that our constraints on F and $\frac{d{\rm REW}_c}{dz}$ are very similar to the results already presented in the paper. We also found good fits for the UV luminosity functions. This gives us confidence that our results are not sensitive to the precise choice of the functional form that was used to model the REW-PDF.

APPENDIX B: CALCULATION OF EW-PDF FOR LYα SELECTED GALAXIES

The EW-PDF of galaxies as a function of Lyα luminosity, is

$$P({\rm REW}|L_\alpha) = \int_0^{-\infty} dM_{\rm UV} P({\rm REW}|L_\alpha, M_{\rm UV})P(M_{\rm UV}|L_\alpha). \tag{B1}$$

Bayes theorem states that

$$P(M_{\rm UV}|L_\alpha) = \frac{P(M_{\rm UV}, L_\alpha)}{P(L_\alpha)} = \frac{P(L_\alpha|M_{\rm UV})P(M_{\rm UV})}{P(L_\alpha)}, \tag{B2}$$

and we may write

$$P({\rm REW}|L_\alpha) = \int_0^{-\infty} dM_{\rm UV} \ P({\rm REW}|L_\alpha, M_{\rm UV})P(L_\alpha|M_{\rm UV})\frac{P(M_{\rm UV})}{P(L_\alpha)}. \tag{B3}$$

We also know that $P(L_\alpha|M_{\rm UV}) = P({\rm REW}|M_{\rm UV})\frac{\partial {\rm REW}}{\partial L_\alpha} = P({\rm REW}|M_{\rm UV})\frac{\rm REW}{L_\alpha}$ (see § 2.1.2). For a particular combination of L_α and $M_{\rm UV}$, the REW is fixed, implying that $P({\rm REW}|L_\alpha, M_{\rm UV}) = \delta_{\rm D}(g(M_{\rm UV})$, where $\delta_D(x)$ denotes the Dirac delta function and $g(M_{\rm UV}) \equiv {\rm REW} - \frac{L_\alpha}{C\times{\rm REW}\times L_{\rm UV,\nu}}$. We can therefore write

$$P({\rm REW}|L_\alpha) = \int_0^{-\infty} dM_{\rm UV} \ \delta_{\rm D}(g(M_{\rm UV}))P(M_{\rm UV})$$
$$\times P({\rm REW}|M_{\rm UV})\frac{\rm REW}{L_\alpha P(L_\alpha)}$$
$$= \frac{P({\rm REW}|M_{\rm UV,c})}{g'(M_{\rm UV,c})}\frac{\rm REW}{L_\alpha P(L_\alpha)}P(M_{\rm UV,c})$$
$$= P({\rm REW}|M_{\rm UV,c})\frac{\rm REW}{L_\alpha P(L_\alpha)}\frac{P(M_{\rm UV,c})}{g'(M_{\rm UV,c})}, \tag{B4}$$

where in the last step we evaluated $g'(M_{\rm UV})$ at the pole of $g(M_{\rm UV})$, i.e. when $C \times {\rm REW} \times 10^{-0.4(M_{\rm UV,c}+s)} \equiv L_\alpha$. We can simplify this further to

$$P({\rm REW}|L_\alpha) = -2.5P({\rm REW}|M_{\rm UV,c})\frac{P(M_{\rm UV,c})}{\ln 10 \ L_\alpha P(L_\alpha)}. \tag{B5}$$

We finally compute the REW-PDF as

$$P({\rm REW}) = \mathcal{N}\int_{L_{\alpha,\rm min}}^{L_{\alpha,\rm max}} dL_\alpha P({\rm REW}|L_\alpha)P(L_\alpha)$$
$$= \mathcal{N}\int_{L_{\alpha,\rm min}}^{L_{\alpha,\rm max}} P({\rm REW}|M_{\rm UV,c})P(M_{\rm UV,c})d\log_{10}L_\alpha \tag{B6}$$

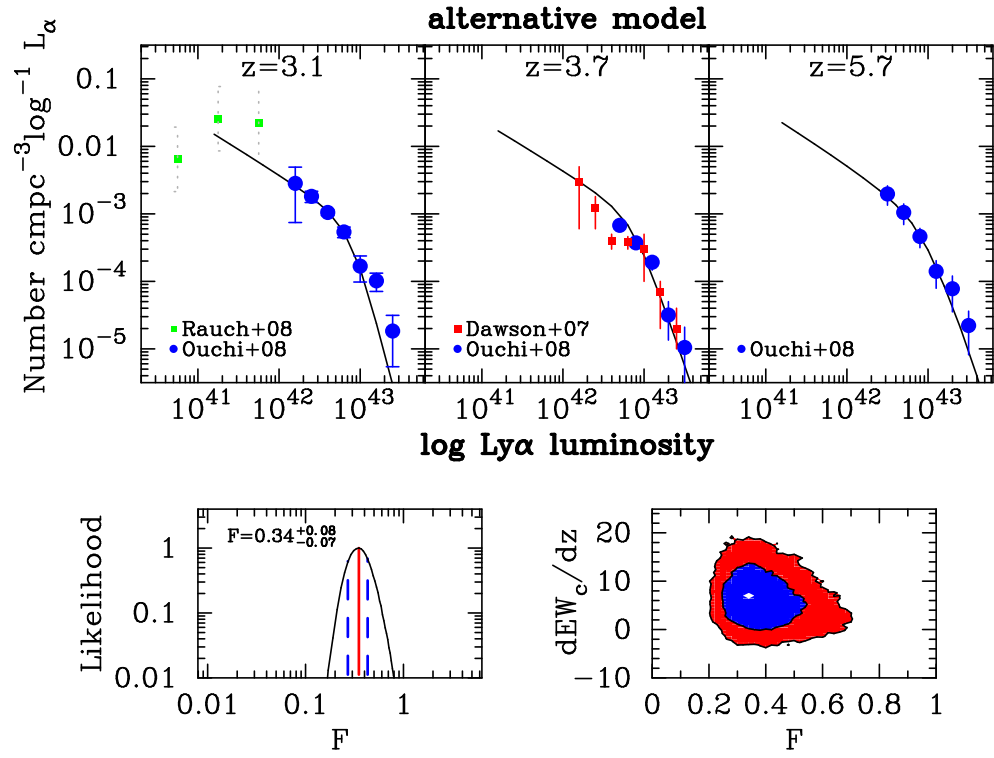where $\mathcal{N}$ is the normalization constant (which absorbed all numerical factors).

Figure A6. Same as Figure 1, but for our alternative parametrization of the REW-PDF. The most likely value for F decreased further from $F = 0.43$ to $F = 0.34$, and $F = 1$ is ruled out at $\gtrsim 99\%$ CL.